AN EXPECTED COMPLIANCE MODEL BASED ON TOPOLOGY OPTIMIZATION FOR DESIGNING STRUCTURES SUBMITTED TO RANDOM LOADS

MIGUEL CARRASCO, BENJAMIN IVORRA, RODRIGO LECAROS,
AND ANGEL MANUEL RAMOS

Dedicated to Professor Jesús Ildefonso Díaz
on the occasion of his 60th birthday

(*Communicated by J.-M. Rakotoson*)

Abstract. In this paper, we focus in developing a stochastic model for topology optimization. The principal objective of such a model is to find robust structures for a given main load having a stochastic behavior. In the first part, we present the expected compliance formulation and some results in topology optimization. Then, in order to illustrate the interest of our approach, we consider a preliminary 3D cantilever benchmark experiment and compare the obtained results with the one given by a single load approach.

1. Introduction

We consider an elastic homogeneous body $\Omega \subseteq \mathbb{R}^d$, where d is either 2 or 3. We impose that in $\Gamma_u \subseteq \partial\Omega$ (boundary of Ω) the displacements of the body are not allowed and we apply some external load forces f to Ω and g to $\Gamma_t \subseteq \partial\Omega$. A graphical representation of Ω and the external forces is given in Figure 1.

In order to simplify the notations, we assume, without loss of generality, that $g = 0$. We note that the results obtained in this paper can be easily extended to the case $g \neq 0$. Furthermore, we consider that our body is composed by a linear material and therefore the displacements can be computed by solving the following system of linear partial differential equations:

$$\begin{cases} -\operatorname{div}(K e(u)) = f & \text{in } \Omega, \\ u = 0 & \text{on } \Gamma_u, \\ (K e(u)) \cdot n = 0 & \text{on } \partial\Omega \setminus \Gamma_u, \end{cases} \tag{1}$$
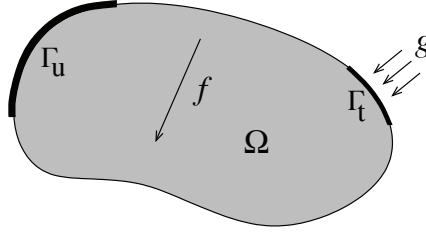
Figure 1: Representation of the elastic homogeneous body Ω and the considered external forces f and g.

where $f : \Omega \to \mathbb{R}^d$ corresponds to an external load, $u : \Omega \to \mathbb{R}^d$ is the vector of displacements, $e(u) = \frac{1}{2}(\nabla u + \nabla u^T)$ denotes the strain tensor and K is the material elasticity tensor (see [12]). Furthermore, under suitable conditions on the data (which are assumed to be satisfied in the rest of the paper), Problem (1) has a unique weak solution (see [8] for more details).

We consider the following function

$$\begin{aligned} \rho : \Omega &\to [\rho_{\min}, \rho_{\max}] \\ x &\mapsto \rho(x) \end{aligned}, \tag{2}$$

which measures the density (i.e., amount) of material at each point of Ω (see [4, 13]), considering a maximum and minimum material density of $\rho_{\max} > 0$ and $\rho_{\min} > 0$, respectively. The total amount of material in Ω, defined by $\int_{\Omega} \rho(x)\,\mathrm{d}x$, must satisfy

$$0 < \int_{\Omega} \rho(x)\,\mathrm{d}x = V_{\mathrm{cons}}. \tag{3}$$

We assume that K depends on the density ρ in the following way (see [4])

$$K = \rho(x)^p K^0,$$

where $p \geqslant 1$ is the penalization power which intends to increase the areas of low (close to $\rho_{\min}$) or high (close to $\rho_{\max}$) density and reduce the medium (between $\rho_{\min}$ and $\rho_{\max}$) density zones, as the material is assumed to be isotropic, K^0 is a matrix of the form

$$K^0_{i,j,k,l} = 2\lambda\,\delta_{i,k}\delta_{j,l} + \mu\delta_{i,j}\delta_{k,l},$$

where $\delta_{i,j}$ denotes the Kronecker symbol and $\lambda, \mu > 0$ are the Lamé constants of the material.

Following [4, 9], we define the functionals

$$A[\rho](u,v) := \int_{\Omega} K_{i,j,k,l}e_{i,j}(u)e_{i,j}(v)\,\mathrm{d}x, \tag{4}$$

$$l(v) := \int_{\Omega} f \cdot v\,\mathrm{d}x. \tag{5}$$

Then, the weak solution of (1) is the vector

$$u \in H = \{u \in [H^1(\Omega)]^d \mid u|_{\Gamma_u} = 0\}$$

($H^1(\Omega)$ is the Sobolev space of all $v \in L^2(\Omega)$ with $\partial_{x_i} v \in L^2(\Omega)$) satisfying

$$A[\rho](u(\rho), v) = l(v), \ \forall v \in H.$$

Thus, the well known minimum compliance design problem can be stated as following

$$\min_{\rho \in E} \ l(u(\rho)), \tag{6}$$

$$\text{such that: } A[\rho](u(\rho), v) = l(v), \quad \text{for all } v \in H, \tag{7}$$

where E is the space of functions satisfying (2) and (3) and $u(\rho)$ denotes the (unique) weak solution of (1).

Here, our purpose is to find the optimal distribution of material ρ when the external load force has a stochastic behavior. In an analogous way to previous stochastic results for truss optimization (see [3, 7]), we assume that the external load force f is randomly perturbed by ξ, with $\mathbb{E}(\xi) = 0$. The stochastic topology design problem can be stated as

$$\min_{\rho \in E} \{\mathbb{E}[\Psi(\xi, \rho)]\}, \tag{8}$$

where the functional Ψ is defined by

$$\Psi(\xi, \rho) = \left\{ \int_{\Omega} (f + \xi) \cdot u \, dx \mid u \in H \text{ satisfies:} \right.$$

$$\left. A[\rho](u, v) = \int_{\Omega} (f + \xi) \cdot v \, dx \text{ for all } v \text{ in } H \right\} \tag{9}$$

and $\mathbb{E}(\cdot)$ denotes the expected value of the corresponding random function.

In this work, we first show that (8) can be rewritten as a multiload problem and thus solved by using optimization algorithms. Then, we illustrate the interest of this approach by considering a 3D benchmark problem and by comparing the obtained results with those given considering Problem (6)-(7).

2. Expected compliance model

In this section, we study the stochastic topology design Problem (9) presented in the introduction. We show that this problem can be transformed into a multiload problem in which the loading scenarios are related to the variance of a random load applied to the body Ω.

In the following, we consider the set $\{P_i\}_{i=1}^{\infty}$ of functions of the Hilbert space $L^2(\Omega)^d$, corresponding to directions of perturbation of the main force f. Also, $\mathscr{B}$ denotes the space of probability and $\mathbb{P}$ its probability measure.

LEMMA 1. *Let* $\xi: \Omega \times \mathscr{B} \to \mathbb{R}^d$ *be a random load, which in terms of the directions of perturbation* $\{P_i\}_{i=1}^{\infty}$ *is written as* $\xi = \sum_1^{\infty} \varepsilon_i P_i$ *where* $(\varepsilon_i)_{i=1}^{\infty} \subset \mathbb{R}$ *are random variables with* $\mathbb{E}(\varepsilon_i) = 0$ *and* $\mathbb{E}(\varepsilon_i \varepsilon_j) = \alpha_{i,j}$ *for* $i,j = 1, \ldots, \infty$. *Let* G *be a linear functional. Then*

$$\mathbb{E}\left(\int_{\Omega} \xi \cdot G(\xi) \, dx\right) = \sum_{i=1}^{+\infty} \sum_{j=1}^{+\infty} \alpha_{i,j} \int_{\Omega} P_i \cdot G(P_j) \, dx.$$

Proof. Using $\xi = \sum_{i=1}^{+\infty} \varepsilon_i P_i$ and Fubini's Theorem we obtain

$$\int_{\Omega} \int_{\mathbb{R}^d} \xi \cdot G(\xi) \, d\mathbb{P} \, dx = \int_{\Omega} \int_{\mathbb{R}^d} \sum_{i=1}^{+\infty} \varepsilon_i P_i \cdot G\left(\sum_{j=1}^{+\infty} \varepsilon_j P_j\right) d\mathbb{P} \, dx$$

$$= \int_{\Omega} \int_{\mathbb{R}^d} \sum_{i=1}^{+\infty} \sum_{j=1}^{+\infty} \varepsilon_i \varepsilon_j P_i \cdot G(P_j) \, d\mathbb{P} \, dx$$

$$= \int_{\Omega} \sum_{i=1}^{+\infty} \sum_{j=1}^{+\infty} \left(\int_{\mathbb{R}^d} \varepsilon_i \varepsilon_j \, d\mathbb{P}\right) P_i \cdot G(P_j) \, dx.$$

$\square$

The following theorem states the relation between the multiload truss model and Problem (9).

THEOREM 1. *Let us consider* $\xi: \Omega \times \mathscr{B} \to \mathbb{R}^d$ *be a random load, which in terms of the directions* $\{P_i\}_{i=1}^{\infty}$ *is written as* $\xi = \sum_1^{\infty} \varepsilon_i P_i$ *where* $(\varepsilon_i)_{i=1}^{\infty}$ *are independent random variables,* $\mathbb{E}(\varepsilon_i \varepsilon_j) = 0$ *for* $i \neq j$, *with* $\mathbb{E}(\varepsilon_i) = 0$ *and* $\text{Var}(\varepsilon_i) = \sigma_i^2$. *Then the stochastic problem defined in* (8) *can be rewritten as the multiload problem:*

$$\min_{\rho \in E} \int_{\Omega} f \cdot u \, dx + \sum_{i=1}^{+\infty} \int_{\Omega} \sigma_i P_i \cdot U_i \, dx, \tag{10}$$

$$A(\rho)[u,v] = \int_{\Omega} f \cdot v \, dx, \; \forall v \in H, \tag{11}$$

$$A(\rho)[U_i,v] = \int_{\Omega} \sigma_i P_i \cdot v \, dx, \; \forall v \in H, \forall \, i \in \mathbb{N}, \tag{12}$$

$$u \in H, U_i \in H \; \forall i \in \mathbb{N}. \tag{13}$$

Proof. Let $\rho \in E$ be a feasible material distribution and let us consider $\xi: \mathbb{R}^d \times \mathscr{B} \to \mathbb{R}$ be a random load with $\mathbb{E}(\xi) = 0$. We define the inverse functional

$$G(f + \xi) = u$$

where u is the unique weak solution of the system (1) changing f by $f + \xi$. The expected value of the compliance is given by

$$\mathbb{E}(\Psi(\xi, \rho)) = \int_{\mathbb{R}^d} \int_{\Omega} (f + \xi) \cdot u \, dx \, d\mathbb{P}.$$

Using Fubini's theorem and linearity of inverse operator G we have

$$
\begin{aligned}
\mathbb{E}(\Psi(\xi,\rho)) &= \int_{\Omega}\int_{\mathbb{R}^d}(f+\xi)\cdot G(f+\xi)\,\mathrm{d}\mathbb{P}\,\mathrm{d}x \\
&= \int_{\Omega}\int_{\mathbb{R}^d}f\cdot G(f)\,\mathrm{d}\mathbb{P}\,\mathrm{d}x + \int_{\Omega}\int_{\mathbb{R}^d}\xi\cdot G(f)\,\mathrm{d}\mathbb{P}\,\mathrm{d}x \\
&\quad + \int_{\Omega}\int_{\mathbb{R}^d}f\cdot G(\xi)\,\mathrm{d}\mathbb{P}\,\mathrm{d}x + \int_{\Omega}\int_{\mathbb{R}^d}\xi\cdot G(\xi)\,\mathrm{d}\mathbb{P}\,\mathrm{d}x \\
&= \int_{\Omega}\mathbb{P}(\mathbb{R}^d)f\cdot G(f)\,\mathrm{d}x + \int_{\Omega}\mathbb{E}(\xi)G(f)\,\mathrm{d}x + \int_{\Omega}G^*(f)\cdot\mathbb{E}(\xi)\,\mathrm{d}x \\
&\quad + \int_{\Omega}\int_{\mathbb{R}^d}\xi\cdot G(\xi)\,\mathrm{d}\mathbb{P}\,\mathrm{d}x \\
&= \int_{\Omega}f\cdot G(f)\,\mathrm{d}x + \int_{\Omega}\int_{\mathbb{R}^d}\xi\cdot G(\xi)\,\mathrm{d}\mathbb{P}\,\mathrm{d}x,
\end{aligned}
$$

where G^* denotes the adjoint operator of G.

Using Lemma 1, and the fact that $\mathbb{E}(\varepsilon_i\varepsilon_j)=0$ for $i\neq j$, we obtain

$$
\int_{\Omega}\int_{\mathbb{R}^d}\xi\cdot G(\xi)\,\mathrm{d}\mathbb{P}\,\mathrm{d}x = \int_{\Omega}\sum_{i=1}^{+\infty}\sigma_i^2 P_i\cdot G(P_i)\,\mathrm{d}x.
$$

Denoting by U_i the unique weak solution of

$$
A(\rho)[U_i,v] = \int_{\Omega}\sigma_i P_i\cdot v\,\mathrm{d}x \text{ for all } v\in H,
$$

we finally get

$$
\mathbb{E}(\Psi(\xi,\rho)) = \int_{\Omega}f\cdot u\,\mathrm{d}x + \int_{\Omega}\sum_{i=1}^{+\infty}\sigma P_i\cdot U_i\,\mathrm{d}x.
$$

$\square$

Theorem 1 is useful because, when its assumptions are satisfied, it gives an explicit expression of Problem (8) easy to evaluate. In general cases, it could be difficult to evaluate directly $\mathbb{E}[\Psi(\xi,\rho)]$. We can consider, for instance, a *Monte-Carlo* algorithm (see [10]) to approximate those values. However, this method, and thus the resolution of (8), is numerically expensive.

In Section 3, we present a numerical experiment used to illustrate the interest of formulation (10).

3. Numerical example

3.1. Problem description

We consider a 3D benchmark design problem that consists in designing a cantilever submitted to a vertical load [4]. More precisely, we consider a rectangular domain $\Omega = [0,25]\times[0,10]\times[0,10]$, compound by a material with a minimum and maximum density of $\rho_{\min}=10^{-3}$ and $\rho_{\max}=10$, respectively. The face $\{0\}\times[0,10]\times$

$[0,10]$ of Ω is fixed to a support area. The total amount of material is $V_{\text{cons}} = 1250$. A main point load $f = (0,0,-1)$ is applied at the node $(25,5,5)$. We consider a random point load $\xi = \xi_1 V_1 + \xi_2 V_2$, with ξ_1 and ξ_2 random variables of law $\mathcal{N}(0,25)$, $V_1 = (1,0,0)$ and $V_2 = (0,1,0)$, applied at the same node than f. We consider the typical value $p = 3$ [13]. A geometrical representation of this benchmark problem is given in Figure 2.
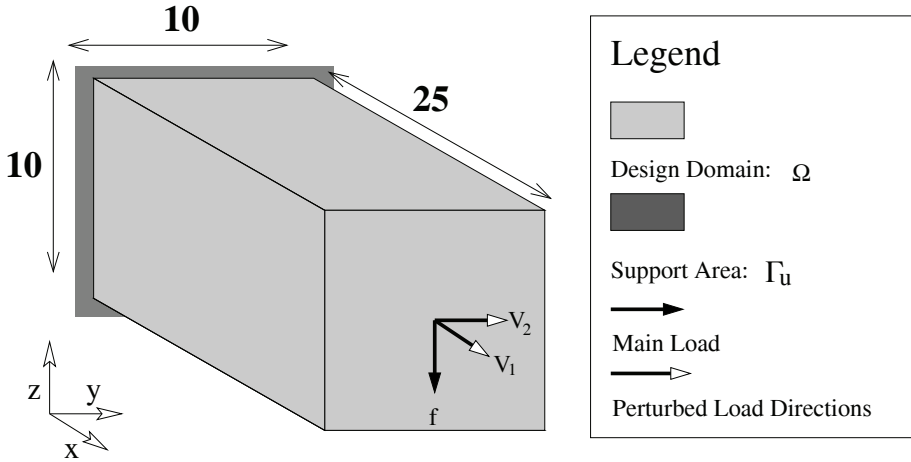

Figure 2: Geometrical representation of the 3D cantilever design problem described in Section 3.1: design domain Ω (gray), support area Γ_u (dark gray), main load f and perturbed load directions V_1 and V_2 (arrows).

We want to solve Problems (6)- (7) and (10)-(13) associated to the cantilever. To do so, we consider a finite element method, similar to the one proposed in [13], with a discretization given by $N_x = 25$, $N_y = 10$ and $N_z = 10$, where N_x, N_y and N_z are the number of equispaced elements in the X, Y and Z directions, respectively. Thus,

$$N_{\text{el}} = N_x \times N_y \times N_z = 2500$$

is the total number of elements used. Then, both optimization problems are solved by using the *Global Optimization Platform* software, freely available at

$$\texttt{http://www.mat.ucm.es/momat/software.htm}$$

with 100 iterations, the steepest descent method as the core algorithm and where the initial condition generated by 5 iterations of a multi-layer secant method. The gradient of the functional to be minimized is approximated with a first order finite difference approach. A complete description and validation of this algorithm can be found in [10, 11]. The obtained solutions are denoted by ρ_{sp} for Problem (6)-(7) and ρ_{ec} for Problem (10)-(13) .

In order to have a qualitative comparison of ρ_{sp} and ρ_{ec}, we analyze their robustness when they are submitted to random loads and their density distribution. For this

purpose, we first compute the compliance value without considering any perturbed load. Then, for each solution $\rho \in \{\rho_{sp}, \rho_{ec}\}$, we consider the random variable $\Phi_\rho = \Psi(\xi, \rho)$. We approximate the density function of Φ_ρ, denoted by γ_{Φ_ρ}, by using a Monte-Carlo approach [10] that generates $M \in \mathbb{N}$ possible *scenarios* (i.e., values of ξ). Then, we calculate some statistical values of γ_{Φ_ρ}: its mean, maximum and 1%-Coherent-Value at Risk (C-VaR$_1$) values.

The ν%-Coherent-Value at Risk (C-VaR) is a risk measure defined as:

$$\text{C-VaR}_\nu(\chi) = \frac{1}{\nu} \int_0^\nu \inf \left\{ z \in \mathbb{R} \text{ s.t.} \int_0^z 100 \rho_\chi(x) dx > (100 - y) \right\} dy,$$

where ν is a percentile, $\chi \in L^\infty(\Omega, \mathscr{A}, \mathbb{P})$ and ρ_χ is the density function of χ. C-VaR$_\nu$ corresponds to the average value of the worst ν % case scenarios of χ (i.e., the ν % highest values of χ). A presentation and an application of C-VaR can be found in [10]. In our case, we have $\chi = \Phi_\rho$.

3.2. Results

Some results found with the numerical experiments presented in Section 3.1 are reported in Table 1. The density distribution of ρ^{sp} and ρ^{ec} are presented in Figures 3 and 4, respectively.

Solution	Compl	EC	C-VaR$_1$	Max
ρ_{sp}	1683	44798	321612	415021
ρ_{ec}	3906	11129	61487	103936
Percent variation	+ 132	-75	-81	-75

Table 1: Results obtained when considering ρ_{sp} and ρ_{ec}: Compliance value (Compl), expected compliance (EC), coherent value at risk (C-VaR$_1$) of Φ_ρ and maximum value (Max) of Φ_ρ. The last line corresponds to the percent variation (%) between the results given by ρ_{sp} and ρ_{ec}.

As we can see on Table 1, the solution ρ_{sp} has a non perturbed compliance value of 1683. The compliance value of ρ_{ec} is 3906 (more than twice higher). However, when considering perturbed loads, the expected compliance, the C-VaR$_1$ and the maximum values of $\Phi_{\rho_{ec}}$ are more than four times lower than those of $\Phi_{\rho_{sp}}$. This result is expected as the distribution ρ_{sp} is adapted to resist to the main load but is less stable to perturbations of f. In counterpart, ρ_{ec} allows to obtain reduced perturbed compliance values. This can also be deduced by observing the shape of both solutions (see Figures 3-4): the density distribution ρ_{sp} is concentrated in the X-Z plane including f, producing a good resistance to the main load, whereas ρ_{ec} exhibits four pillars resilient to the perturbed loads included in the X-Y plane orthogonal to f.
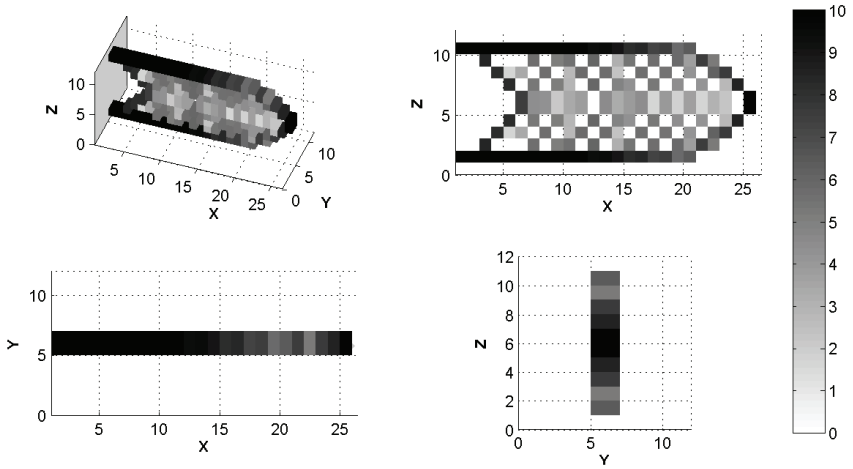
Figure 3: Shape and density distribution of ρ_{sp}: (Top-Left) Perspective view with representation of the support area (gray plane), (Top-Right) Lateral view (i.e., *X-Z* plane), (Bottom-Left) Top view (i.e., *X-Y* plane) and (Bottom-Right) Face view (i.e., *Y-Z* plane). The gray scale color map representing the density is also presented.

Figure 4: Shape and density distribution of ρ_{ec}: (Top-Left) Perspective view with representation of the support area (gray plane), (Top-Right) Lateral view (i.e., *X-Z* plane), (Bottom-Left) Top view (i.e., *X-Y* plane) and (Bottom-Right) Face view (i.e., *Y-Z* plane). The gray scale color map representing the density is also presented.
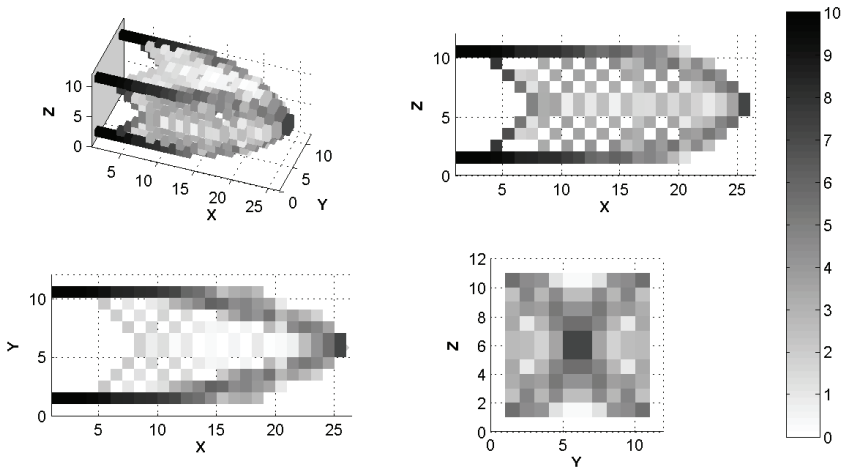
From this preliminary result, as in the truss optimization case studied in [7], we can deduce that considering formulation (10) for topology optimization can help to generate structures robust to perturbations of the main load.

4. Conclusions

We have adapted an expected compliance formulation, coming from truss design (see [3, 7]), to topology optimization. We have exhibited, in a particular case, an explicit expression easy to evaluate. This method has been tested numerically on a 3D benchmark test case. This approach allows to generate structures that are more stable to perturbations of the main load than considering a classical non perturbed load approach. In a future work, the results given in this paper will be extended by performing more numerical experiments. Then, as in the truss case, we will include the variance of the compliance in our model to create improved structures.

REFERENCES

[1] W. ACHTZIGER, *Topology optimization of discrete structures: an introduction in view of computational and nonsmooth aspects*, In Topology optimization in structural mechanics, volume 374 of CISM Courses and Lectures, pages 57–100, Springer, Vienna, 1997.

[2] W. ACHTZIGER, M. BENDSØE, A. BEN-TAL, AND J. ZOWE, *Equivalent displacement based formulations for maximum strength truss topology design*, Impact Comput. Sci. Engrg., **4**, 4 (1992), 315–345.

[3] F. ALVAREZ AND M. CARRASCO, *Minimization of the expected compliance as an alternative approach to multiload truss optimization*, Struct. Multidiscip. Optim., **29**, 6 (2005), 470–476.

[4] M. P. BENDSØE AND O. SIGMUND, *Topology optimization. Theory, methods and applications*, Springer-Verlag, Berlin, 2003.

[5] A. BEN-TAL AND A. NEMIROVSKI, *Robust truss topology design via semidefinite programming*, SIAM J. Optim., **7**, 4 (1997), 991–1016.

[6] A. BEN-TAL AND M. ZIBULEVSKY, *Penalty/barrier multiplier methods for convex programming problems*, SIAM J. Optim., **7** 2 (1997), 347–366.

[7] M. CARRASCO, B. IVORRA AND A.M. RAMOS, *A variance-expected compliance model for structural optimization*, Journal of Optimization Theory and Applications, accepted, 2011.

[8] P. CIARLET, *Mathematical Elasticity*, Vol. I, Three Dimensional Elasticity, North-Holland, Amsterdam, 1988.

[9] S. CONTI, H. HELD, M. PACH, M. RUMPF AND R. SCHULTZ, *Shape optimization under uncertainty, a stochastic programming perspective*, SIAM Journal on Optimization, **19**, 4 (2008), 1610–1632.

[10] B. IVORRA, B. MOHAMMADI, AND A.M. RAMOS, *Optimization strategies in credit portfolio management*, Journal Of Global Optimization, **43** 2 (2009), 415–427.

[11] B. IVORRA, A. M. RAMOS, AND B. MOHAMMADI, *Semideterministic global optimization method: Application to a control problem of the Burgers equation*, Journal of Optimization Theory and Applications, **135**, 3 (2007), 549–561.

[12] L. D. LANDAU, E. M. LIFSHITZ, *Theory of Elasticity*, Oxford, England: Butterworth Heinemann, 1986.

[13] O. SIGMUND, *A* 99 *line topology optimization code written in Matlab*, Structural and Multidisciplinary Optimization, **21**, 2 (2001), 120–127.

Differential Equations & Applications
www.ele-math.com
dea@ele-math.com

Miguel Carrasco
Facultad de Ingeniería
Universidad de los Andes
Av. San Carlos de Apoquindo 2200, Santiago de Chile
Chile
e-mail: `migucarr@uandes.cl`

Benjamin Ivorra
Departamento de Matemática Aplicada
Universidad Complutense de Madrid &
Instituto de Matemática Interdisciplinar
Plaza de Ciencias, 3, 28040–Madrid
Spain
e-mail: `ivorra@mat.ucm.es`

Rodrigo Lecaros
Departamento de Ingeniería Matemática
Facultad de Ingeniería, Universidad de Chile
Blanco Encalada 2120, Santiago de Chile
Chile
e-mail: `rlecaros@dim.uchile.cl`

Angel Manuel Ramos
Departamento de Matemática Aplicada
Universidad Complutense de Madrid &
Instituto de Matemática Interdisciplinar
Plaza de Ciencias, 3, 28040–Madrid
Spain
e-mail: `angel@mat.ucm.es`

Differential Equations & Applications
www.ele-math.com
dea@ele-math.com